

The Unique Application of AFM/SCM-2D-Carrier Profiling Through Thick Insulating Layers

Kuo-Jen Chao

Charles Evans & Associates - Member of the Evans Analytical Group, 810 Kifer Road, Sunnyvale, CA 94086, USA

ABSTRACT

- Atomic force microscopy [1] and scanning capacitance microscopy [2] (AFM/SCM) have been applied to study various implant structures of semiconductor devices. In this work, we present a unique application of AFM/SCM in 2D-carrier profiling through a thick insulating layer. Many researchers have applied various 2D-profiling techniques (such as Scanning Spreading Resistance Microscopy, SSRM) to study cross-sectional semiconductor devices to delineate the dopant (or carrier) profiles in the source and drain regions and further determine the channel length. However, most techniques can only probe the dopant (or carrier) profiles on the surface or direct near-surface regions. They typically encounter significant difficulties in delineating the dopant (or carrier) profiles at depths larger than a few hundred Å from the top surface.
- Here we demonstrate the unique ability of AFM/SCM in delineating the carrier distribution two-dimensionally 1000Å below the top surface. The sample is a GaAs substrate masked by a 1000Å thick layer of Si₃N₄. Patterns were etched into the Si₃N₄ layer to expose the GaAs substrate. Then Zn dopants were thermally diffused through the openings in the nitride layer into the substrate. Simultaneously acquired AFM and SCM images of a line-opening clearly reveal the carrier distributions beneath the 1000Å thick nitride layer. Overlaying the AFM and SCM images reveals the lateral diffusion length of the Zn dopants to be about 2.2 μm from the edges of the exposed GaAs region.
- This work demonstrates the utility of AFM/SCM in process control and failure analysis. Three failed Si devices analyzed by SCM for failure analysis are presented.

INTRODUCTION

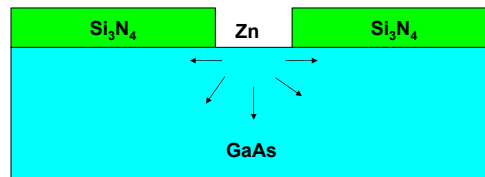
- Atomic force microscopy [1] and scanning capacitance microscopy [2] (AFM/SCM) have been applied to study various implant structures of semiconductor devices. The primary focus is to quantitatively delineate the dopant concentration two-dimensionally in the source/drain regions at the channel of the silicon metal-oxide-semiconductor field effect transistors (MOSFETs) from the SCM image acquired on the cross-sectioned surface of the device [3-5]. In addition to SCM, various analytical techniques have also been developed to perform 2D-profiling [2,5-12] in an attempt to meet the requirements of the dopant profiling stated in the International Technology Roadmap for Semiconductors (ITRS). It is not the purpose of this research to find solutions for AFM/SCM to provide better quantitative accuracy or higher lateral resolution in 2-D dopant profiles, but only to apply its strength (carrier profiling capability) as a complementary analysis tool in semiconductor manufacturing processes.
- SCM is operated by using the AFM to perform capacitance measurements on semiconductor materials, where the conductive coating on the AFM probe serves as the metal element of the metal-insulator-semiconductor (MIS) device, but on a much smaller scale. A number of factors complicate the SCM measurement including: 1) the sample surface smoothness and the oxide (or insulator) quality, 2) the tip size and shape, 3) the stray light from the AFM laser, and 4) the stray capacitance, etc [13]. The key challenges in minimizing these factors are that the device dimensions that need to be monitored are on the order or even smaller than the resolutions of most analytical techniques. To determine **qualitative** 2-D carrier distribution, the influence of these factors would be either minimized or negligible by acquiring SCM images on top-down insulator on semiconductor devices rather than on cross-sectioned devices.
- In this study, AFM/SCM measurements were obtained directly from the top surfaces of the insulator-on-semiconductor samples. The unique ability of AFM/SCM in delineating the carrier distribution two-dimensionally through a thick insulating layer is demonstrated. This unique capability makes AFM/SCM very useful in process control and device failure analyses. AFM/SCM was further applied to determine the influence of the mask shapes on the geometry of the lateral dopant distributions. Finally, direct applications in failure analyses are presented.

EXPERIMENTAL

- Digital Instruments' (Santa Barbara, CA) NanoScope III Dimension 5000/Large Sample Stage AFM/SCM System
- AFM and SCM images are acquired simultaneously.
- The AFM image is on the left while the SCM image is on the right.
- Process Control: two GaAs samples
- Failure Analyses: three failed Si devices

PROCESS CONTROL

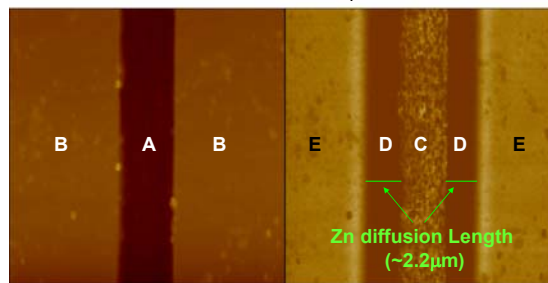
Determination of Lateral Dopant Distribution



- Two GaAs samples: #1 and #2.
- GaAs substrates with a 1000Å thick Si₃N₄ overlayer.
- Various patterns of the Si₃N₄ layer were etched away to expose the substrate.
- Zn dopants were thermally diffused through the openings of the nitride (Si₃N₄) layer into the exposed GaAs substrate.
- Sample #1: a straight-line pattern.
- Sample #2:
 - pattern a: obtuse corners
 - pattern b: acute corners

Probing through a 1000Å thick layer

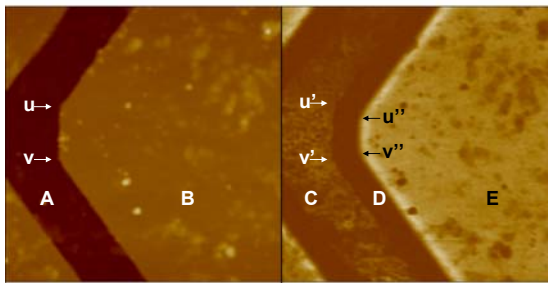
Determination of Lateral Dopant Distribution



- AFM (Left)/SCM (Right) images of Sample #1.
- (A): the exposed GaAs substrate, (B): the Si₃N₄ surfaces, (C): the exposed GaAs substrate, (D): the Zn diffused GaAs region, and (E): undoped GaAs region.
- The lateral diffusion length of the Zn dopant is about 2.2 μm.
- SCM successfully detected carrier variation even at a depth of more than 1000Å from the tip of the probe.**

Edge Corner Influence on Lateral Dopant Distribution

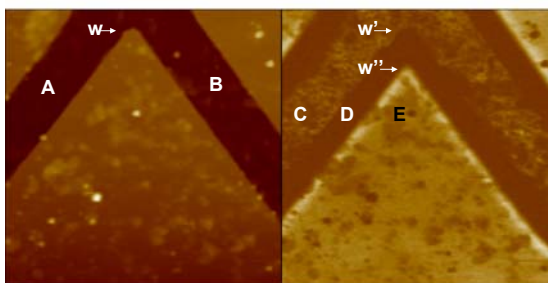
Obtuse Corner



- AFM (Left)/SCM (Right) images of a 25μm x 25μm area of pattern a (Obtuse Corner) of Sample #2.
- (A): the exposed GaAs substrate, (B): the Si₃N₄ surfaces, (C): the exposed GaAs substrate, (D): the Zn diffused GaAs region, and (E): undoped GaAs region.
- The edge corners (u'' and v'') of the dopant diffused area are rounder than the edge corner (u and v) of the Si₃N₄ mask.
- An obtuse corner of the mask generally results in a rounder corner of the dopant diffused region.**

Edge Corner Influence on Lateral Dopant Distribution

Acute Corner



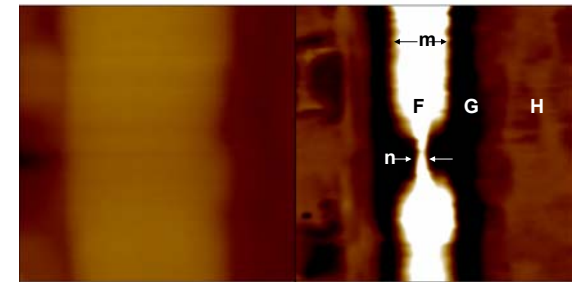
- AFM(Left)/SCM(Right) images of a 25μm x 25μm area of pattern b (Acute Corner) of Sample #2.
- (A): the exposed GaAs substrate, (B): the Si₃N₄ surfaces, (C): the exposed GaAs substrate, (D): the Zn diffused GaAs region, and (E): undoped GaAs region.
- The edge corner (w'') of the dopant diffused area is sharper than the edge corner (w) of the Si₃N₄ mask.
- An acute corner of the mask results in a sharper corner of the dopant diffused region.**
- A useful formula for engineering the geometry of the lateral dopant distribution:
 - An obtuse corner of the mask generally results in a rounder corner of the dopant diffused region.
 - An acute corner of the mask results in a sharper corner of the dopant diffused region.

FAILURE ANALYSIS

- Three failed Si devices were deprocessed for a top-down study to find the root causes of the failures.

Failure Analysis Example #1

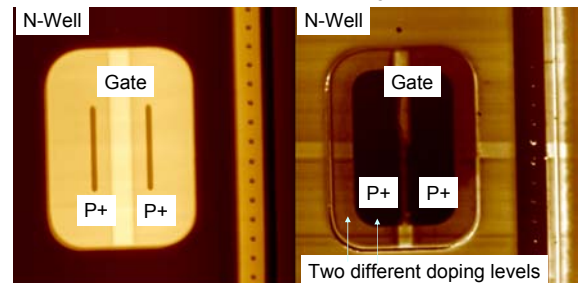
Non-uniform Gate Width



- AFM/SCM images of a failed deprocessed Si device #1.
- (Left) AFM top view of a 1.5μm x 1.5μm area
- (Right) SCM image of the same area
- While the width of the white region 'm' is mostly uniform (about 0.3μm), a small fraction of it 'n' is about 0.06μm.

Failure Analysis Example #2

Inappropriate Doping



- AFM/SCM images of a failed deprocessed Si device #2.
- (Left) AFM top of a 23.5μm x 23.5μm area.
- (Right) SCM image of the same area.
- Two different doping levels are observed in the intended P+ regions.

Failure Analysis Example #3

Unexpected Bridging



- AFM/SCM images of a failed deprocessed Si device #3.
- (Left) AFM top of a 35.5μm x 35.5μm area.
- (Right) SCM image of the same area.
- Region B bridges regions A and C.

SUMMARY

- A unique 2D-carrier profiling capability of SCM was presented: **SCM is able to detect carrier concentration through a 1000Å thick insulating layer.**
- Influences of the mask geometry on the lateral dopant diffusions are analyzed.
 - a rounder corner of the dopant diffused area results from an obtuse corner of the mask.
 - a sharper corner of the dopant diffused area results from an acute corner of the mask.
- Failure mechanisms of three defective Si devices are analyzed and determined by AFM/SCM.

ACKNOWLEDGEMENT

The author would like to thank **Thomas Fister** for useful and helpful suggestions and discussions.

REFERENCES

- G. Binnig, C. F. Quate, and C. Gerber, Phys. Rev. Lett. **56**, pp. 930-933, 1986.
- C. C. Williams, W. P. Hough, and S. A. Rishton, Appl. Phys. Lett. **55**, 203 (1989).
- A. C. Diebold, M. R. Kump, J. J. Kopanski, and D. G. Seiler, J. Vac. Sci. Technol. B **14**, 196 (1996).
- J. J. Kopanski, J. F. Marchiando, and J. R. Lowmey, J. Vac. Sci. Technol. B **14**, 242 (1996).
- N. Duhayon, P. Eyben, M. Fouchier, T. Clarysse, W. Vandervorst, D. Alvarez, S. Schoemann, M. Ciappa, M. Stangoni, W. Fichtner, P. Formanek, M. Kittler, V. Raineri, F. Giannazzo, D. Goghero, Y. Rosenwaks, R. Shikler, S. Saraf, S. Sadewasser, N. Barreau, T. Glatzel, M. Verheijen, S. A. M. Mentink, M. von Sprekelsen, T. Maltezos, and R. Wiesendanger, J. Vac. Sci. Technol. B **22**, 385 (2004).
- G. A. Cooke, P. Pearson, R. Gibbons, M. G. Dowsett, and C. Hill, J. Vac. Sci. Technol. B **14**, 348 (1996).
- P. De Wolf, T. Clarysse, W. Vandervorst, J. Snauwaert, and L. Hellemans, J. Vac. Sci. Technol. B **14**, 380 (1996).
- M. Barrett, M. Dennis, D. Tiffin, Y. Li, and C. K. Shih, J. Vac. Sci. Technol. B **14**, 447 (1996).
- D. Venables and D. M. Maher, J. Vac. Sci. Technol. B **14**, 421 (1996).
- K.-J. Chao, A. R. Smith, A. J. McDonald, D.-L. Kwong, B. Streetman, and C. K. Shih, J. Vac. Sci. Technol. B **16**, 453 (1998).
- H. Edwards, R. McGlothlin, R. S. Martin, E. U. M. Grnbelyuk, R. Mahaffy, C. K. Shih, R. S. List, and V. A. Ukraintsev, Appl. Phys. Lett. **72**, 698 (1998).
- F. Y. Liu, P. B. Griffin, J. D. Plummer, J. W. Lyding, J. M. Moran, J. F. Richards, and L. Kulig, J. Vac. Sci. Technol. B **22**, 422 (2004).
- J. J. Kopanski, J. F. Marchiando, B. G. Rennex, D. Simons, and Q. Chau, J. Vac. Sci. Technol. B **22**, 399 (2004).